Water Supply

IWA PUBLISHING

Water Supply Vol 22 No 4, 4193 doi: 10.2166/ws.2022.044

Experimental and numerical study of flow at a 90 degree lateral turnout with enhanced roughness coefficient and invert level changes

Maryam Bagheri[a], Seyed M. Ali Zomorodian[b], Masih Zolghadr[c], H. Md. Azamathulla[d,*] and C. Venkata Siva Rama Prasad[e]

[a] Hydraulic Structures, Department of Water Engineering, Shiraz University, Shiraz, Iran
[b] Department of Water Engineering, College of Agriculture, Shiraz University, Shiraz, Iran
[c] Department of Water Sciences Engineering, College of Agriculture, Jahrom University, Jahrom, Iran
[d] Civil & Environmental Engineering, The University of the West Indies, St. Augustine Campus, Port of Spain, Trinidad
[e] Department of Civil Engineering, St. Peters Engineering College, Hyderabad, India
*Corresponding author. E-mail: azmatheditor@gmail.com

HMA, 0000-0002-5436-4147

ABSTRACT

Flow separation at the upstream side of lateral turnouts (intakes) is a critical issue causing eddy currents at the turnout entrance. It reduces the effective width of flow, turnout capacity and efficiency. Therefore, it is essential to identify the dimensions of the separation zone and propose remedies to reduce its dimensions. Installation of 7 types of roughening elements at the turnout entrance and 3 different bed invert levels, with 4 different discharges (making a total of 84 experiments) were examined in this study as a method to reduce the dimensions of the separation zone. Additionally, a 3-D Computational Fluid Dynamic (CFD) model was utilized to evaluate the flow pattern and dimensions of the separation zone. Results showed that enhancing the roughness coefficient can reduce the separation zone dimensions up to 38% while the drop implementation effect can scale down this area differently based on the roughness coefficient used. Combining both methods can reduce the separation zone dimensions up to 63%.

Key words: discharge ratio, flow separation zone, intake, three dimensional simulation

HIGHLIGHTS

- Flow separation at the upstream side of lateral turnouts (intakes) is a critical issue causing eddy currents at the turnout entrance.
- Installation of 7 types of roughening elements at the turnout entrance and 3 different bed level inverts were investigated.
- Additionally, a 3-D Computational Fluid Dynamic (CFD) model was utilized to evaluate the flow.
- Combining both methods can reduce the separation zone dimensions by up to 63%.

GRAPHICAL ABSTRACT

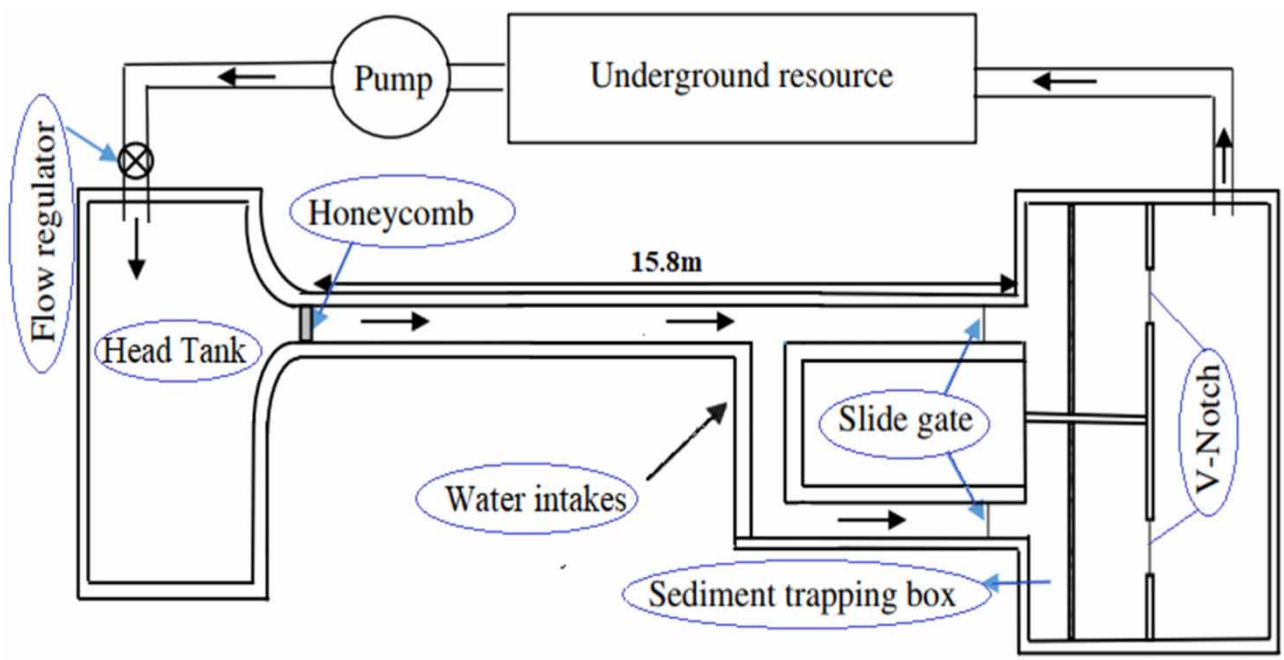

INTRODUCTION

Turnouts or intakes are amongst the oldest and most widely used hydraulic structures in irrigation networks. Turnouts are also used in water distribution, transmission networks, power generation facilities, and waste water treatment plants etc. The flows that enter a turnout have a strong momentum in the direction of the main waterway and that is why flow separation occurs inside the turnout. The horizontal vortex formed in the separation area is a suitable place for accumulation and deposition of sediments. The separation zone is a vulnerable area for sedimentation and for reduction of effective flow due to a contracted flow region in the lateral channel. Sedimentaion in the entrance of the intake can gradually be transfered into the lateral channel and decrease the capacity of the higher order channels over time (Jalili *et al.* 2011). On the other hand, the existence of coarse-grained materials causes erosion and destruction of the waterway side walls and bottom. In addition, sedimentation creates conditions for vegetation to take root and damage the waterway cover, which causes water to leak from its perimeter. Therefore, it is important to investigate the pattern of the flow separation area in turnouts and provide solutions to reduce the dimensions of this area.

The three-dimensional flow structure at turnouts is quite complex. In an experimental study by Neary & Odgaard (1993) in a 90-degree water turnout it was found that the secondary currents and separation zone varies from the bed to the water surface. They also found that at a 90-degree water turnout, the bed roughness and discharge ratio play a critical role in flow structure. They asserted that an explanation of sediment behavior at a diversion entrance requires a comprehensive understanding of 3D flow patterns around the lateral-channel entrance. In addition, they suggested that there is a strong similarity between flow in a channel bend and a diversion channel, and that this similarity can rationalize the use of bend flow models for estimation of 3D flow structures in diversion channels.

Some of the distinctive characteristics of dividing flow in a turnout include a zone of separation immediately near the entrance of the lateral turnout (separation zone), a contracted flow region in the branch channel (contracted flow), and a stagnation point near the downstream corner of the junction (stagnation zone). In the region downstream of the junction, along the continuous far wall, separation due to flow expansion may occur (Ramamurthy *et al.* 2007), that is, a separation zone. This can both reduce the turnout efficiency and the effective width of flow while increasing the sediment deposition in the turnout entrance (Jalili *et al.* 2011). Installation of submerged vanes in the turnout entrance is a method which is already applied to reduce the size of flow separation zones. The separation zone draws sediments and floating materials into themselves. This reduces effective cross-section area and reduces transmission capacity. These results have also been obtained in past studies,

including by Ramamurthy *et al.* (2007) and in Jalili *et al.* (2011). Submerged vanes (Iowa vanes) are designed in order to modify the near-bed flow pattern and bed-sediment motion in the transverse direction of the river. The vanes are installed vertically on the channel bed, at an angle of attack which is usually oriented at 10–25 degrees to the local primary flow direction. Vane height is typically 0.2–0.5 times the local water depth during design flow conditions and vane length is 2–3 times its height (Odgaard & Wang 1991). They are vortex-generating devices that generate secondary circulation, thereby redistributing sediment within the channel cross section. Several factors affect the flow separation zone such as the ratio of lateral turnout discharge to main channel discharge, angle of lateral channel with respect to the main channel flow direction and size of applied submerged vanes. Nakato *et al.* (1990) found that sediment management using submerged vanes in the turnout entrance to Station 3 of the Council Bluffs plant, located on the Missouri River, is applicable and efficient. The results show submerged vanes are an appropriate solution for reduction of sediment deposition in a turnout entrance. The flow was treated as 3D and tests results were obtained for the flow characteristics of dividing flows in a 90-degree sharp-edged, junction. The main and lateral channel were rectangular with the same dimensions (Ramamurthy *et al.*, 2007).

Keshavarzi & Habibi (2005) carried out experiments on intake with angles of 45, 67, 79 and 90 degrees in different discharge ratios and reported the optimum angle for inlet flow with the lowest flow separation area to be about 55 degrees. The predicted flow characteristics were validated using experimental data. The results indicated that the width and length of the separation zone increases with the increase in the discharge ratio Qr (ratio of outflow per unit width in the turnout to inflow per unit width in the main channel).

Abbasi *et al.* (2004) performed experiments to investigate the dimensions of the flow separation zone at a lateral turnout entrance. They demonstrated that the length and width of the separation zone decreases with the increasing ratio of lateral turn-out discharge. They also found that with a reducing angle of lateral turnout, the length of the separation zone scales up and width of separation zone reduces. Then they compared their observations with results of Kasthuri & Pundarikanthan (1987) who conducted some experiments in an open-channel junction formed by channels of equal width and an angle of lateral 90 degree turnout, which showed the dimensions of the separation zone in their experiments to be smaller than in previous studies. Kasthuri & Pundarikanthan (1987) studied vortex and flow separation dimensions at the entrance of a 90 degree channel. Results showed that increasing the diversion discharge ratio can reduce the length and width of the vortex area. They also showed that the length and width of the vortex area remain constant at diversion ratios greater than 0.7. Karami Moghaddam & Keshavarzi (2007) analyzed the flow characteristics in turnouts with angles of 55 and 90 degrees. They reported that the dimensions of the separation zone decrease by increasing the discharge ratio and reducing the turnout angle with respect to the main channel. Studies about flow separation zone can be found in Jalili *et al.* (2011), Nikbin & Borghei (2011), Seyedian *et al.* (2008).

Jamshidi *et al.* (2016) measured the dimensions of a flow separation zone in the presence of submerged vanes with five arrangements (parallel, stagger, compound, piney and butterflies). Results showed that the ratio of the width to the length of the separation zone (shape index) was between 0.2 and 0.28 for all arrangements.

Karami *et al.* (2017) developed a 3D computational fluid dynamic (CFD) code which was calibrated by measured data. They used the model to evaluate flow pattern, diversion ratio of discharge, strength of the secondary flow, and dimensions of the vortex inside the channel in various dikes and submerged vane installation scenarios. Results showed that the diversion ratio of discharge in the diversion channel is dependent on the width of the flow separation area in the main channel. A dike, perpendicular to the flow, doubles the ratio of diverted discharge and reduces the suspended sediment load compared with the base-line situation by creating outer arch conditions. In addition, increasing the longitudinal distance between vanes increases the velocity gradient between the vanes and leads to a more severe erosion of the bed near the vanes.

Al-Zubaidy & Hilo (2021) used the Navier–Stokes equation to study the flow of incompressible fluids. Using the CFD software ANSYS Fluent 19.2, 3D flow patterns were simulated at a diversion channel. Their results showed good agreement using the comparison between the experimental and numerical results when the k-omega turbulence viscous model was employed. Simulation of the flow pattern was then done at the lateral channel junction using a variety of geometry designs. These improvements included changing the intake's inclination angle and chamfering and rounding the inner corner of the intake mouth instead of the sharp edge. Flow parameters at the diversion including velocity streamlines, bed shear stress, and separation zone dimensions were computed in their study. The findings demonstrated that changing the 90° lateral intake geometry can improve the flow pattern and bed shear stress at the intake junction. Consequently, sedimentation and erosion problems are reduced. According to the conclusions of their study, a branching angle of 30° to 45° is the best configuration for increasing branching channel discharge, lowering branching channel sediment concentration.

The review of the literature shows that most of the studies deal with turnout angle, discharge ratio and implementation of vanes as techniques to reduce the area of the separation zone. This study examines the effect of roughness coefficient and drop implementation at the entrance of a 90-degree lateral turnout on the dimensions of the separation zone. As far as the authors are aware, these two variables have never been studied as a remedy to decrease the separation zone dimensions whilst enhancing turnout efficiency. Additionally, a three-dimensional numerical model is applied to simulate the flow pattern around the turnout. The numerical results are verified against experimental data.

METHOD

Experimental setup

The experiments were conducted in a 90 degree dividing flow laboratory channel. The main channel is 15 m long, 0.5 m wide and 0.4 m high and the branch channel is 3 m long, 0.35 m wide and 0.4 m high, as shown in Figure 1. The tests were carried out at 9.65 m from the beginning of the flume and were far enough from the inlet, so we were sure that the flow was fully developed. According to Kirkgöz & Ardiçlioğlu (1997) the length of the developing region would be approximantly 65 and 72 times the flow depth. In this study, the depth is 9 cm, which makes this condition.

Both the main and lateral channel had a slope of 0.0003 with side walls of concrete. A 100 hp pump discharged the water into a stilling basin at the entrance of the main flume. The discharge was measured using an ultrasonic discharge meter around the discharge pipe. Eighty-four experiments in total were carried out at range of $0.1<Fr<0.4$ (Froude numbers in main channel and upstream of turnout). The depth of water in the main channel in the experiments was 9 cm, in which case the effect of surface tension can be considered; according to research by Zolghadr & Shafai Bejestan (2020) and Zolghadr *et al.* (2021), when the water depth is more than 6 cm, the effect of surface tension is reduced and can be ignored given that the separation phenomenon occurs in the boundary layer, the height of the roughness creates disturbances in growth and development of the boundary layer and, as a result, separation growth is also faced with disruption and its dimensions grow less compared to smooth surfaces. Similar conditions occur in case of drop implementation. A disturbance occurs in the growth of the boundary layer and as a result the separation zone dimensions decrease. In order to investigate the effect of roughness coefficient and drop implementation on the separation zone dimensions, four different discharges (16, 18, 21, 23 l/s) in subcritical conditions, seven Manning (Strickler) roughness coefficients (0.009, 0.011, 0.017, 0.023, 0.028, 0.030, 0.032) as shown in Figure 2 and three invert elevation differences between the main channel and lateral turnout invert (0, 5 and 10 cm) at the entrance of the turnout were considered. The Manning roughness coefficient values were selected based on available and feasible values for real conditions, so that 0.009 is equivalent to galvanized sheet roughness and selected for the baseline tests. 0.011 is for concrete with neat surface, 0.017 and 0.023 are for unfinished and gunite concrete respectively. 0.030 and 0.032 values are for concrete on irregular excavated rock (Chow 1959). The roughness coefficients were created by gluing sediment particles on a thin galvanized sheet which was installed at the upstream side of the lateral turnout. The values of roughness coefficients were calculated based on the Manning-Strickler formula. For this purpose, some uniformly graded sediment samples were prepared and the Manning roughness coefficient of each sample was determined

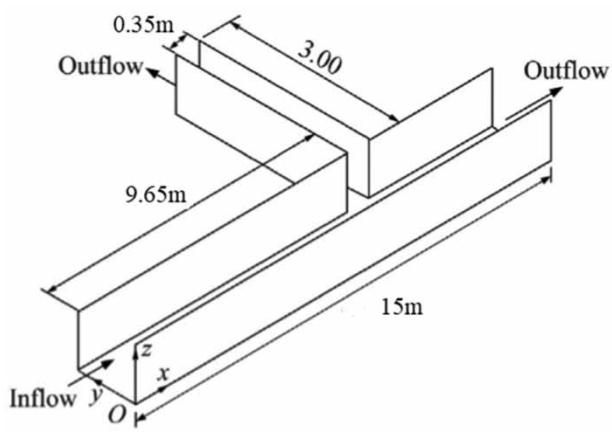

Figure 1 | Laboratory channel dimensions.

Figure 2 | Roughness plates.

with respect to the median size (D_{50}) value pasted into the Manning-Strickler formula. Some $KMnO_4$ was sifted in the main channel upstream to visualize and measure the dimensions of the separation zone. Consequently, when $KMnO_4$ approached the lateral turnout a photo of the separation zone was taken from a top view. All the experiments were recorded and several photos were taken during the experiment after stablishment of steady flow conditions. The photos were then imported to AutoCAD to measure the separation zone dimensions. Because all the shooting was done with a high-definition camera and it was possible to zoom in, the results are very accurate.

The velocity values were also recorded by a one-dimensional velocity meter at 15 cm distance from the turnout entrance and in transverse direction (perpendicular to the flow direction).

The water level was also measured by depth gauges with a accuracy of 0.1 mm, and velocity in one direction with a single-dimensional KENEK LP 1100 with an accuracy of ± 0.02 m/s (0–1 m/s), $\pm$ 0.04 m/s (1–2 m/s), $\pm$ 0.08 m/s (2–4 m/s), ± 0.10 m/s (4–5 m/s).

Numerical simulation

A FLOW-3D numerical model was utilized as a solver of the Navier-Stokes equation to simulate the three-dimensional flow field at the entrance of the turnout. The governing equations included continuity momentum equations. The continuity equation, regardless of the density of the fluid in the form of Cartesian coordinates x, y, and z, is as follows:

$$V_F \frac{\partial \rho}{\partial t} + \frac{\partial}{\partial x}(uA_x) + \frac{\partial}{\partial y} vA_y + \frac{\partial}{\partial z}(wA_z) = \frac{R_{sor}}{\rho} \tag{1}$$

where u, v, and w represent the velocity components in the x, y, and z directions, respectively; A_x, A_y, and A_z are the surface flow fractions in the x, y, and z directions, respectively; V_F denotes flow volume fraction; r is the density of the fluid; t is time; and R_{sor} refers to the source of the mass. Equations (2)–(4) show momentum equations in x, y and z dimensions respectively :

$$\frac{\partial u}{\partial t}\frac{1}{V_F} uA_x \frac{\partial u}{\partial x} + vA_y \frac{\partial u}{\partial y} + wAz \frac{\partial u}{\partial z} = -\frac{1}{\rho}\frac{\partial \rho}{\partial x} + G_x + f_x \tag{2}$$

$$\frac{\partial v}{\partial t}\frac{1}{V_F} uA_x \frac{\partial v}{\partial x} + vA_y \frac{\partial v}{\partial y} + wAz \frac{\partial v}{\partial z} = -\frac{1}{\rho}\frac{\partial \rho}{\partial y} + G_y + f_y \tag{3}$$

$$\frac{\partial w}{\partial t}\frac{1}{V_F} uA_x \frac{\partial w}{\partial x} + vA_y \frac{\partial w}{\partial y} + wAz \frac{\partial w}{\partial z} = -\frac{1}{\rho}\frac{\partial \rho}{\partial z} + G_z + f_z \tag{4}$$

where G_x, G_y, and G_z are the accelerations caused by gravity in the x, y, and z directions, respectively; and f_x, f_y, and f_z are the accelerations caused by viscosity in the x, y, and z directions, respectively.

The turbulence models used in this study were the renormalized group (RNG) models. Evaluation of the concordance of the mentioned models with experimental studies showed that the RNG model provides more accurate results.

Two blocks of mesh were used to simulate the main channels and lateral turnout. The meshes were denser in the vicinity of the entrance of the turnout in order to increase the accuracy of computations. Boundary conditions for the main mesh block included inflow for the channel entrance (volumetric flow rate), outflow for the channel exit, 'wall' for the bed and the right boundary and 'symmetry' for the top (free surface) and left boundaries (turnout). The side wall roughness coefficient was given to the software as the Manning number in surface roughness of any component. Considering the restrictions in the available processor, a main mesh block with appropriate mesh size was defined to simulate the main flow field in the channel, while the nested mesh-block technique was utilized to create a very dense solution field near the roughness plate in order to provide accurate results around the plates and near the entrance of the lateral turnout. This technique reduced the number of required mesh elements by up to 60% in comparison with the method in which the mesh size of the main solution field was decreased to the required extent.

The numerical outputs are verified against experimental data. The hydraulic characteristics of the experiment are shown in Table 1.

RESULTS AND DISCUSSION

Experimental results

During the experiments, the dimensions of the separation zone were recorded with an HD camera. Some photos were imported to AutoCad software. Then, the separation zones dimensions were measured and compared in different scenarios.

At the beginning, the flow pattern in the separation zone for four different hydraulic conditions was studied for seven different Manning roughness coefficients from 0.009 to 0.032. To compare the obtained results, roughness of 0.009 was considered as the base line. The percentage of reduction in separation zone area in different roughness coefficients is shown in Figure 3. According to this figure, by increasing the roughness of the turnout side wall, the separation zone area ratio reduces (ratio of separation zone area to turnout area). In other words, in any desired Froud number, the highest dimensions of the separation zone area are related to the lowest roughness coefficients. In Figure 3, 'A' is the area of the separation zone and 'A_i' represents the total area of the turnout.

It should be mentioned that the separation zone dimensions change with depth, so that the area is larger at the surface than near the bed. This study measured the dimensions of this area at the surface. Figure 4 show exactly where the roughness elements were located.

Figure 5 shows images of the separation zone at n=0.023 and n=0.032 as examples, and show that the separation area at n=0.032 is smaller than that of n=0.023.

The difference between the effect of the two 0.032 and 0.030 roughnesses is minor. In other words, the dimensions of the separation zone decreased by increasing roughness up to 0.030 and then remained with negligable changes.

In the next step, the effect of intake invert relative to the main stream (drop) on the dimensions of the separation zone was investigated. To do this, three different invert levels were considered: (1) without drop; (2) a 5 cm drop between the main canal and intake canal; and (3) a 10 cm drop between the main canal and intake canal. The without drop mode was considered as the control state. Figure 6 shows the effect of drop implementation on separation zone dimensions. Tables 2 and 3 show the reduced percentage of separation zone areas in 5 and 10 cm drop compared to no drop conditions as the base line. It was found that the best results were obtained when a 10 cm drop was implemented.

Table 1 | Hydraulic conditions of the flow

Q(L/s)	Fr	Y_1 (m)	Q_2/Q_1
16	0.449	0.09	0.22
18	0.335	0.09	0.61
21	0.242	0.09	0.71
23	0.180	0.09	1.04

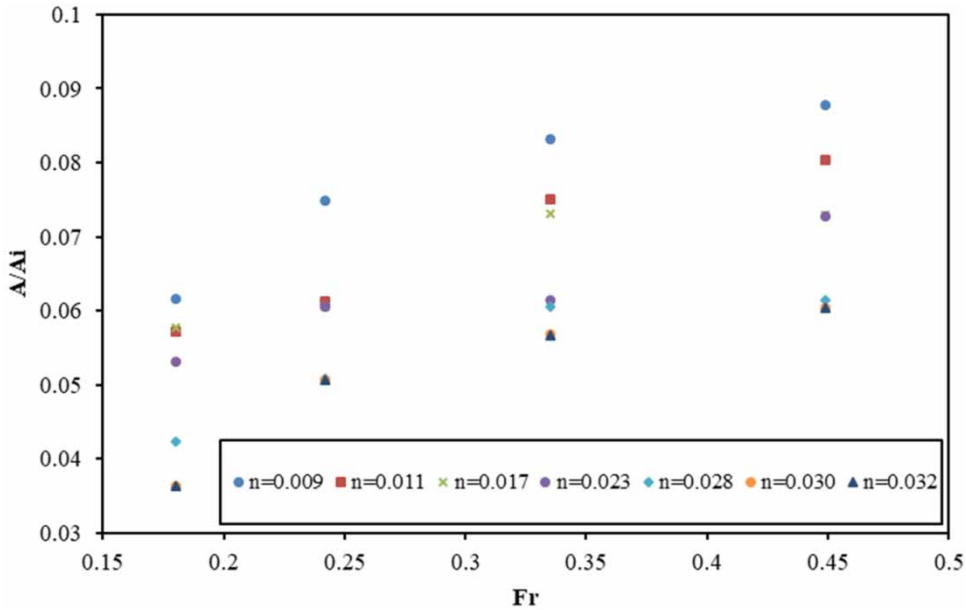

Figure 3 | Effect of roughness on separation zone dimensions.

Figure 4 | Effect of roughness on separation zone dimensions.

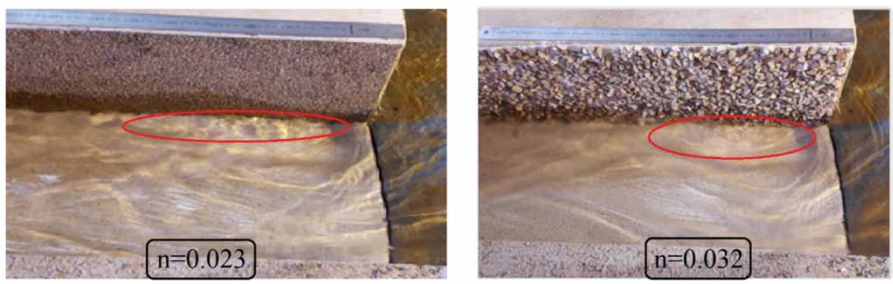

Figure 5 | Comparison of separation zone for n=0.023 and n=0.032.

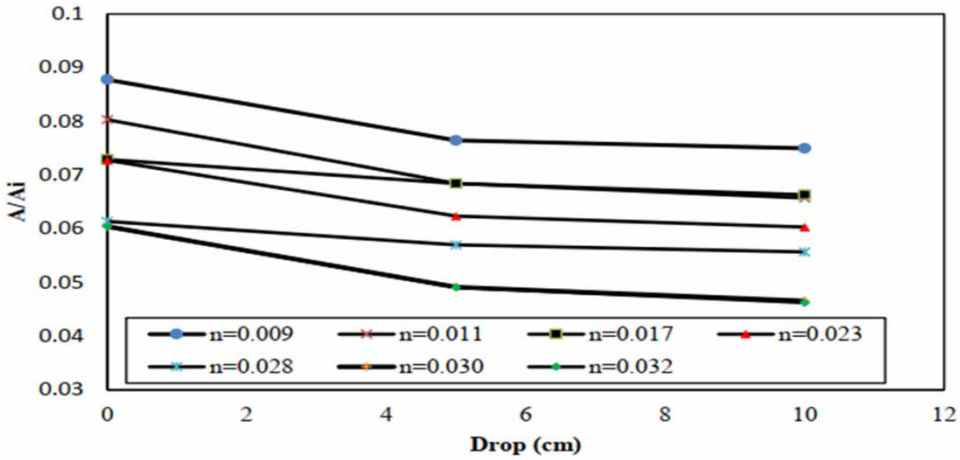

Figure 6 | Effect of drop implementation on separation zone dimensions.

Table 2 | Decrease percentage of separation zone area in 5 cm drop

Fr	n=0.011	n=0.017	n=0.023	n=0.028	n=0.030	n=0.032
0.08	10.56	11.06	25.27	33.03	35.57	36.5
0.121	7.66	11.14	11.88	15.93	34.59	36.25
0.353	1.38	2.63	8.17	14.39	31.20	31.29
0.362	3	11.54	19.56	25.73	37.89	38.31

Table 3 | Decrease percentage of separation zone area in 10 cm drop

Fr	n=0.011	n=0.017	n=0.023	n=0.028	n=0.030	n=0.032
0.047	4.30	8.75	23.47	31.22	34.96	35.13
0.119	11.01	13.16	15.02	21.48	39.45	40.68
0.348	3.89	5.71	9.82	16.09	29	30.96
0.354	2.84	10.44	18.42	25.45	35.68	35.76

The combined effect of drop and roughness is shown in Figure 7. According to this figure, by installing a drop structure at the entrance of the intake, the dimensions of the separation zone scales down in any desired roughness coefficient. Results indicated that by increasing the roughness coefficient or drop implementation individually, the separation zone area decreases up to 38 and 25% respectively. However, employing both techniques simultaneously can reduce the separation zone area up to 63% (Table 4). The reason for the reduction of the dimensions of the separation zone area by drop implementation can be attributed to the increase of discharge ratio. This reduces the dimensions of the separation zone area.

This method increases the discharge ratio (ratio of turnout to main channel discharge). The results are compatible with the literature. Some other researchers reported that increasing the discharge ratio can scale down the separation zone dimensions (Karami Moghaddam & Keshavarzi 2007; Ramamurthy *et al.* 2007). However, these researchers employed other methods to enhance the discharge ratio. Drop implementation is simple and applicable in practice, since there is normally an elevation difference between the main and lateral canal in irrigation networks to ensure gravity flow occurance.

Table 4 depicts the decrease in percentage of the separation zone compared to base line conditions in different arrangements of the combined tests.

A comparison between the proposed methods introduced in this paper and traditional methods such as installation of submerged vanes, and changing the inlet geometry (angle, radius) was performed. Figure 8 shows the comparison of the results.

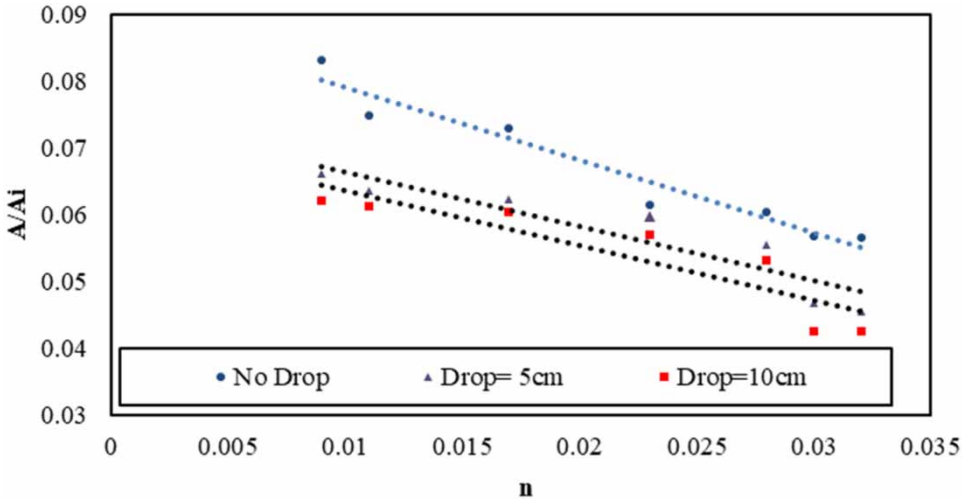

Figure 7 | Combined effect of roughness and drop on separation zone dimensions.

Table 4 | Reduction in percentage of combined effect of roughness and 10 cm drop

Qi	n=0.011	n=0.017	n=0.023	n=0.028	n=0.030	n=0.032
16	32.3	35.07	37.2	45.7	58.01	59.1
18	44.5	34.15	36.18	48.13	54.2	56.18
21	43.18	32.33	42.30	37.79	57.16	63.2
23	40.56	34.5	34.09	46.25	50.12	57.2

The comparison shows that the new techniques can be highly influential and still practical. In this research, with no change in structural geometry (enhancement of roughness coefficient) or minor changes with respect to drop implementation, the dimensions of the separation zone are decreased noticeably. The velocity values were also recorded by a one-dimensional velocity meter at 15 cm distance from the turnout entrance and in a transverse direction (perpendicular to the flow direction). The results are shown in Figure 9.

Numerical results

This study examined the flow patterns around the entrance of a diversion channel due to various wall roughnesses in the diversion channel. Results indicated that increasing the discharge ratio in the main channel and diversion channel reduces the area of the separation zone in the diversion channel.

A laboratory and numerical error rate of 0.2605 was calculated from the following formula,

$$E = \sqrt{\sum (U\exp - Unum)^2 / N}$$

where U_{exp} is the experimental result, Unum is the numerical result, and N is the number of data.

Figure 9 shows the effect of roughness on separation zone dimensions in numerical study. Figure 10 compares the vortex area (software output) for three roughnesses, 0.009, 0.023 and 0.032 and Figure 11 shows the flow lines (tecplot output) that indicate the effect of roughness on flow in the separation zone. Numerical analysis shows that by increasing the roughness coefficient, the dimensions of the separation zone area decrease, as shown in Figure 10 where the separation zone area at n=0.032 is less than the separation zone area at n=0.009.

The velocities intensified moving midway toward the turnout showing that the effective area is scaled down. The velocity values were almost equal to zero near the side walls as expected. As shown in Figure 12 the approach vortex area velocity decreases. Experimental and numerical measured velocity at x=0.15 m of the diversion channel compared in Figure 13

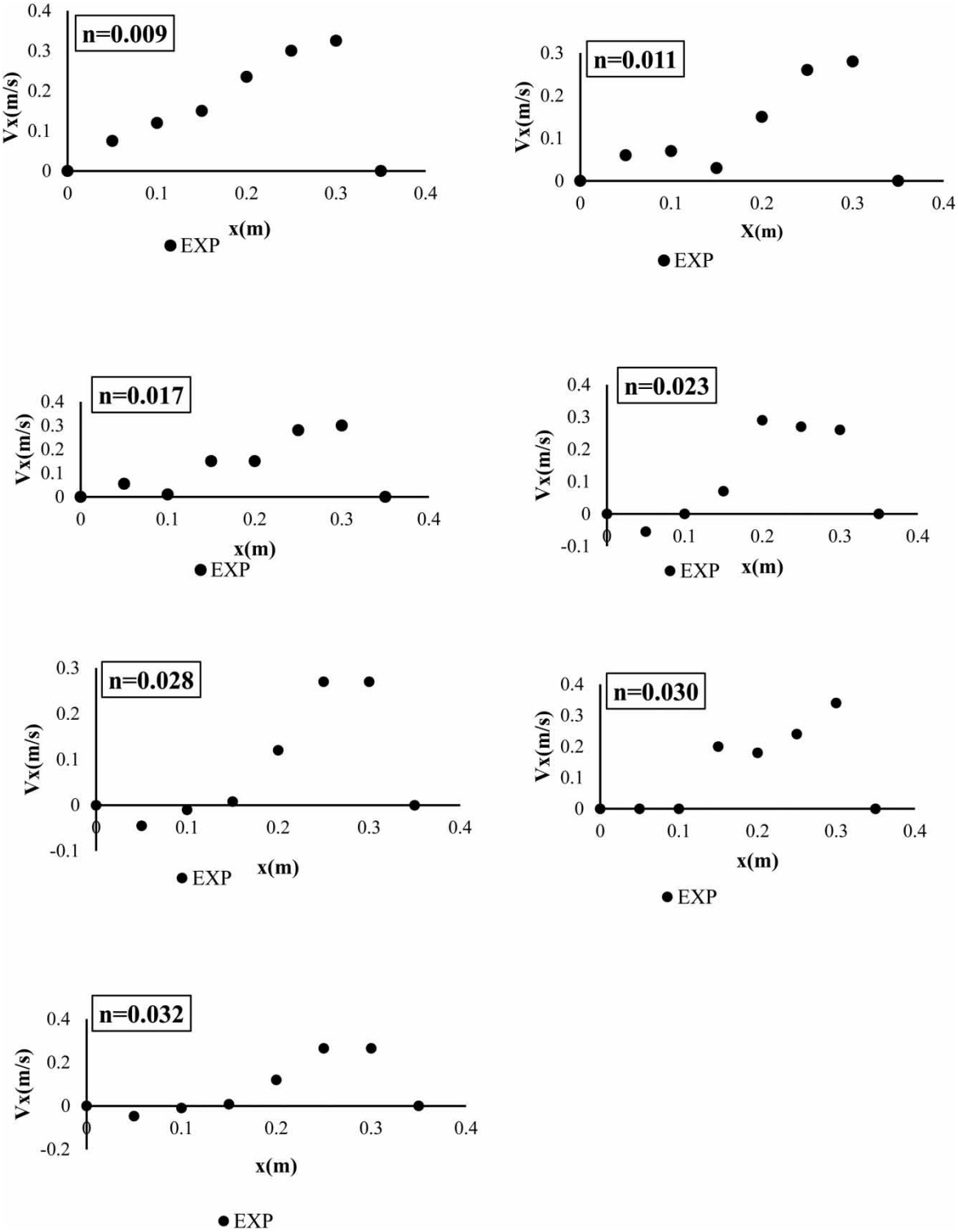

Figure 8 | Velocity profiles for various roughness coefficients along turnout width.

shows that away from the separation zone area, the velocity increases. All longitudinal velocity contours near the vortex area are distinctly different between different roughnesses. The separation zone is larger at less roughness both in length and width.

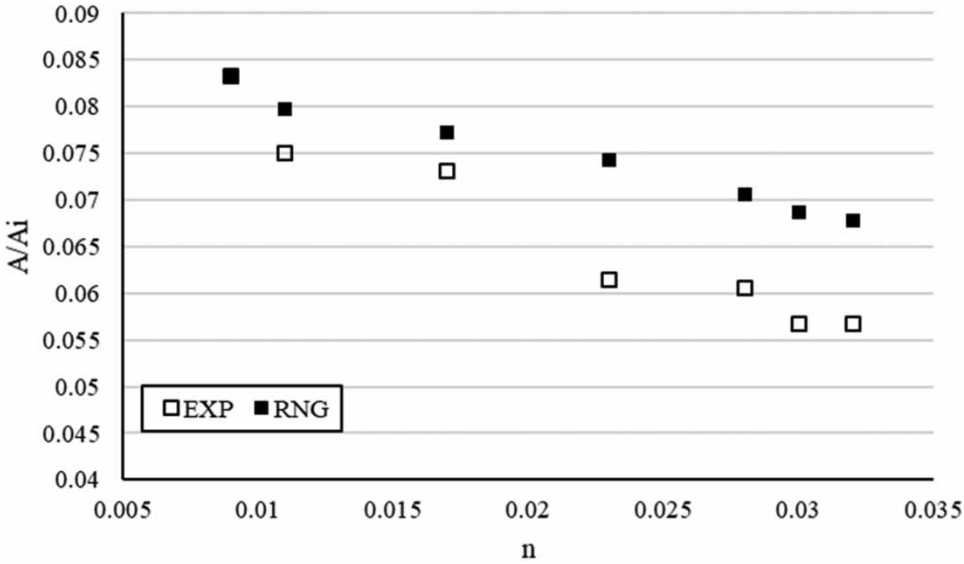

Figure 9 | Effect of roughness on separation zone dimensions in numerical study.

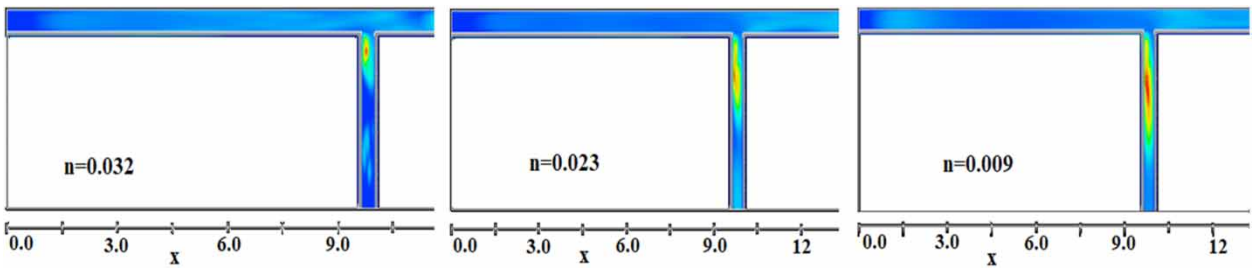

Figure 10 | Comparision of the vortex area (software output) for three roughnesses (0.009, 0.023 and 0.032).

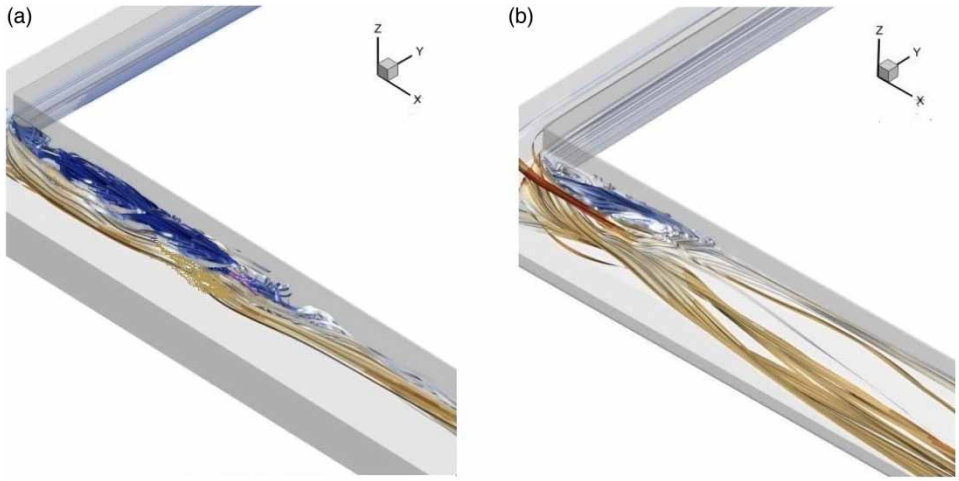

Figure 11 | Comparison of vortex area in 3D mode (tecplot output) with two roughnesses (a) 0.009 and (b) 0.032.

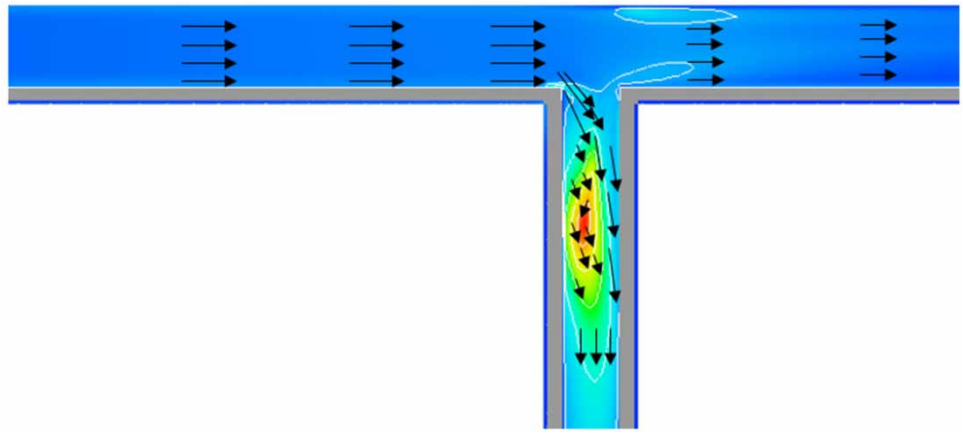

Figure 12 | Velocity vector for flow condition Q¼22 l/s, near surface.

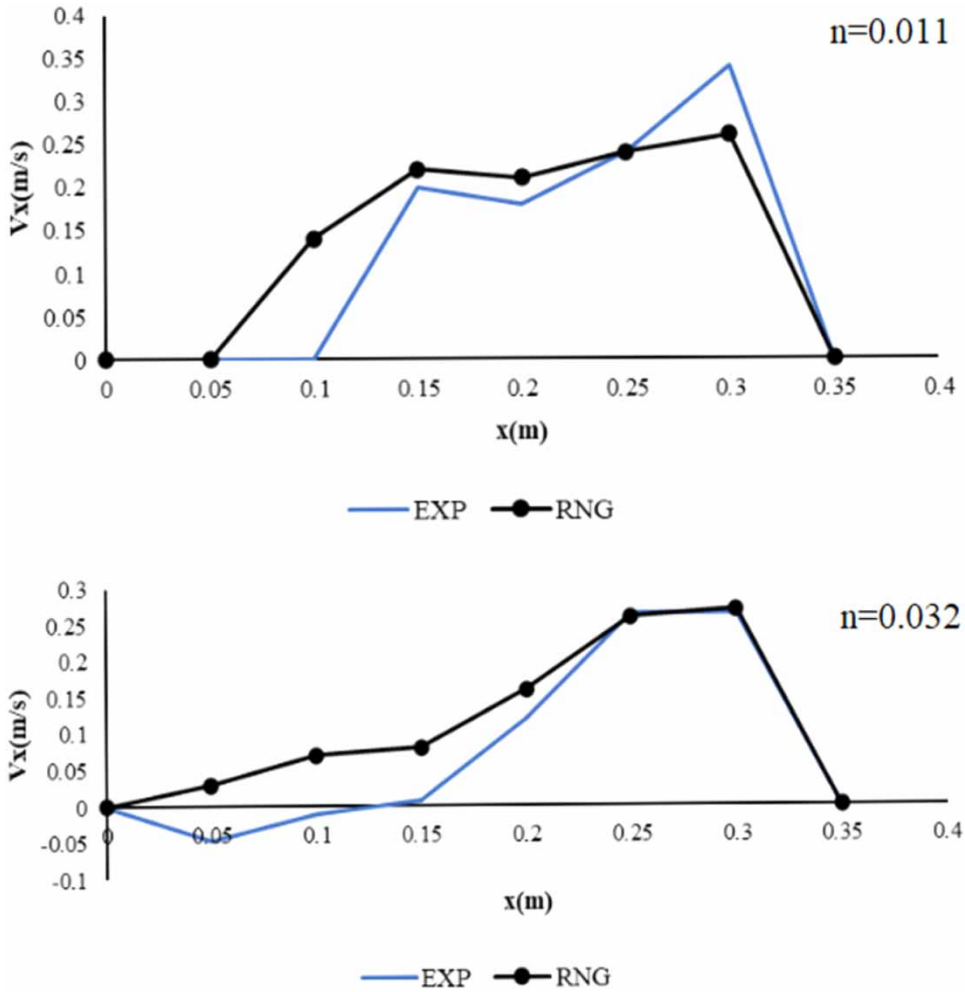

Figure 13 | Exprimental and numerical measured velocity.

CONCLUSION

This study introduces practical and feasible methods for enhancing turnout efficiency by reducing the separation zone dimensions. Increasing the roughness coefficient and implementation of inlet drop were considered as remedies for reduction of separation zone dimensions. A data set has been compiled that fully describes the complex, 3D flow conditions present in a 90 degree turnout channel for selected flow conditions. The aim of this numerical model was to compare the results of a laboratory model in the area of the separation zone and velocity. Results showed that enhancing roughness coefficient reduce the separation zone dimensions up to 38% while the drop implementation effect can scale down this area differently based on roughness coefficient used. Combining both methods can reduce the separation zone dimensions up to 63%. Further research is proposed to investigate the effect of roughness and drop implementation on sedimentation pattern at lateral turnouts. The dimensions of the separation zone decreases with the increase of the non-dimensional parameter, due to the reduction ratio of turnout discharge increasing in all the experiments.

This method increases the discharge ratio (ratio of turnout to main channel discharge). The results are compatible with the literature. Other researchers have reported that intensifying the discharge ratio can scale down the separation zone dimensions (Karami Moghaddam & Keshavarzi 2007; Ramamurthy *et al.* 2007). However, they employed other methods to enhance the discharge ratio. Employing both techniques simultaneously can decrease the separation zone dimensions up to 63%. A comparison between the new methods introduced in this paper and traditional methods such as installation of submerged vanes, and changing the inlet geometry (angle, radius) was performed. The comparison shows that the new techniques can be highly influential and still practical. The numerical and laboratory models are in good agreement and show that the method used in this study has been effective in reducing the separation area. This method is simple, economical and can prevent sediment deposition in the intake canal. Results show that CFD prediction of the fluid through the separation zone at the canal intake can be predicted reasonably well and the RNG model offers the best results in terms of predictability.

DATA AVAILABILITY STATEMENT

All relevant data are included in the paper or its Supplementary Information.

REFERENCES

Abbasi, A., Ghodsian, M., Habibi, M. & Salehi Neishabouri, S. A. 2004 Experimental investigation on dimensions of flow separation zone at lateral intakeentrance. *Research & Construction; Pajouhesh va Sazandegi* **62**, 38–44. (In Persian).

Al-Zubaidy, R. & Hilo, A. 2021 Numerical investigation of flow behavior at the lateral intake using Computational Fluid Dynamics (CFD). *Materials Today: Proceedings*. https://doi.org/10.1016/j.matpr.2021.11.172.

Chow, V. T. 1959 *Open Channel Hydraulics*. McGraw-Hill, New York.

Jalili, H., Hosseinzadeh Dalir, A. & Farsadizadeh, D. 2011 Effect of intake geometry on the sediment transport and lateral flow pattern. *Iranian Water Research Journal* **5** (9), 1–10. (In Persian).

Jamshidi, A., Farsadizadeh, D. & Hosseinzadeh Dalir, A. 2016 Variations of flow separation zone at lateral intake entrance using submerged vanes. *Journal of Civil Engineering Urban* **6** (3), 54–63. Journal homepage. Available from: www.ojceu.ir/main.

Karami Moghaddam, K. & Keshavarzi, A. 2007 Investigation of flow structure in lateral intakes of 55° and 90° with rounded entrance edge. In: *03 National Congress on Civil Engineering University of Tabriz*. Available from: https://civilica.com/doc/16317. (In Persian).

Karami, H., Farzin, S., Sadrabadi, M. T. & Moazeni, H. 2017 Simulation of flow pattern at rectangular lateral intake with different dike and submerged vane scenarios. *Journal of Water Science and Engineering* **10** (3), 246–255. https://doi.org/10.1016/j.wse.2017.10.001.

Kasthuri, B. & Pundarikanthan, N. V. 1987 Discussion on separation zone at open- channel junction. *Journal of Hydraulic Engineering* **113** (4), 543–548.

Keshavarzi, A. & Habibi, L. 2005 Optimizing water intake angle by flow separation analysis. *Journal of Irrigation and Drain* **54**, 543–552. https://doi.org/10.1002/ird.207.

Kirkgöz, M. S. & Ardiçlioğlu, M. 1997 Velocity profiles of developing and developed open channel flow. *Journal of Hydraulic Engineering* 1099–1105. 10.1061/(ASCE)0733-9429(1997)123:12(1099).

Nakato, T., Kennedy, J. F. & Bauerly, D. 1990 Pumpstation intake-shoaling control with submerge vanes. *Journal of Hydraulic Engineering*. https://doi.org/10.1061/(ASCE)0733-9429(1990)116:1(119).

Neary, V. S. & Odgaard, J. A. 1993 Three-dimensional flow structure at open channel diversions. *Journal of Hydraulic Engineering. ASCE* **119** (11), 1224–1230. https://doi.org/10.1061/(ASCE)0733-9429(1993)119:11(1223).

Nikbin, S. & Borghei, S. M. 2011 Experimental investigation of submerged vanes effect on dimensions of flow separation zone at a 90° openchannel junction. In: *06rd National Congress on Civil Engineering University of Semnan*. (In Persian). Available from: https://civilica.com/doc/120494.

Odgaard, J. A. & Wang, Y. 1991 Sediment management with submerged vanes, I: theory. *Journal of Hydraulic Engineering* **117** (3), 267–283.

Ramamurthy, A. S., Junying, Q. & Diep, V. 2007 Numerical and experimental study of dividing open-channel flows. *Journal of Hydraulic Engineering*. See: https://doi.org/10.1061/(ASCE)0733-9429(2007)133:10(1135).

Seyedian, S., Karami Moghaddam, K. & Shafai Begestan, M. 2008 Determining the optimal radius in lateral intakes of 55° and 90° using variation of flow velocity. In: *07th Iranian Hydraulic Conference*. Power & Water University of Technology (PWUT). (In Persian). Available from: https://civilica.com/doc/56251.

Zolghadr, M. & Shafai Bejestan, M. 2020 Six legged concrete (SLC) elements as scour countermeasures at wing wall bridge abutments. *International Journal of River Basin Management*. doi: 10.1080/15715124.2020.1726357.

Zolghadr, M., Zomorodian, S. M. A., Shabani, R. & Azamatulla Md., H. 2021 Migration of sand mining pit in rivers: an experimental, numerical and case study. *Measurement*. https://doi.org/10.1016/j.measurement.2020.108944.

First received 7 September 2021; accepted in revised form 24 January 2022. Available online 4 February 2022